

Enhancement of wastewater treatment using novel laser-made Ti/SnO₂-Sb anodes with improved electrocatalytic properties

Géssica O. S. Santos ^(1,2), Aline R. Dória ^(1,2), Vanessa M. Vasconcelos ⁽¹⁾, Cristina Sáez ⁽³⁾,

Manuel A. Rodrigo ⁽³⁾, Katlin I. B. Eguiluz ^(1,2,*), Giancarlo R. Salazar-Banda ^(1,2)

¹ Electrochemistry and Nanotechnology Laboratory, Institute of Technology and Research (ITP), Aracaju-SE, Brazil.

² Postgraduate Program in Process Engineering (PEP), Tiradentes University, Aracaju-SE, Brazil

³ Chemical Engineering Department, Faculty of Chemical Sciences and Technologies, Universidad Castilla-La Mancha, Ciudad Real, Spain

***Corresponding author:** katlinbarrios@gmail.com

1 **Abstract**

2 In this study, a novel Ti/SnO₂-Sb anode, improved using a laser heating manufacturing
3 procedure, was applied in wastewater treatment. For comparison purposes, similar anodes
4 were manufactured using the conventional furnace heating procedure. Electrochemical
5 characterizations in the background electrolyte confirmed that the novel material has
6 improved electric conductivity, as compared to the furnace-made one and, hence, it may lead
7 to much lower operating costs in real applications. The electrocatalytic properties of the novel
8 anode in comparison with the conventional were evaluated using a standard and well-known
9 reaction: the phenol oxidation. Different operational conditions were evaluated.
10 Concentrations of phenol were monitored by HPLC and analysis of organic matter by TOC
11 analyzer. The best condition of phenol removal was associated with a relatively low energy
12 consumption of 0.80 kWh (gTOC)⁻¹ and specific electrical energy consumption of 0.81 kWh
13 m⁻³ order⁻¹. Interestingly, the phenol is not completely removed after 60 min of treatment
14 using the furnace-made anode under the same operating conditions in which was fully
15 depleted with the new electrode. Moreover, chlorinated by-products remained in the final
16 solution with the conventional electrode and were exhausted with the novel one. Finally, after
17 an extensive comparison with literature about the oxidation of phenol, the Ti/SnO₂-Sb
18 produced by laser-manufacturing procedure presented the best phenol removal as compared
19 with both non-active and active anodes.

20

21

22

23

24

25 **Keywords:** MMO anode; water treatment; electrochemical treatment; phenol.

26

27 **1. Introduction**

28 Electrochemical oxidation (EO) stands out as a promising alternative for wastewater
29 treatment, due to its attractive advantages, such as versatility, ease of operation, and being
30 environmentally friendly. In this technology, the oxidation of recalcitrant or bio-refractory
31 pollutants can occur following two routes: direct electron transfer or indirect mediated
32 oxidation in the bulk solution (Radjenovic and Sedlak, 2015; Moreira et al., 2017). In the
33 direct oxidation, the pollutant can be oxidized directly on the anode surface. Sometimes,
34 oxidation via hydroxyl radicals ($\bullet\text{OH}$) electrogenerated by the electrolysis of the water is also
35 considered as direct (although it is a mediated process) because both the electron transfer
36 mechanisms and the oxidation via hydroxyl radicals cannot be distinguished in bulk
37 electrolysis. In the hydroxyl radical's mechanism, the combustion of the organics to CO_2 and
38 H_2O is favored with an extremely low generation of intermediates. On the other hand, in other
39 indirect oxidation mechanisms, the pollutants are oxidized by the electrogenerated oxidative
40 species, and in this route, the conversion of organics into more oxidized intermediates is
41 favored before reaching mineralization (Marselli et al., 2003).

42 The efficiency of EO depends on many factors. Among them, it is worth mentioning
43 the catalytic anode material (Wu et al., 2014; Martínez-Huitle et al., 2015). $\text{Ti/SnO}_2\text{-Sb}$
44 anodes are among the most studied non-active anodes, due to its low cost and high
45 overpotential for the oxygen evolution reaction, which leads to excellent performance in the
46 oxidation of organic compounds, associated to the generation of weakly bonded (physisorbed)
47 hydroxyl radicals ($\bullet\text{OH}$) (Rao and Venkatarangaiah, 2014; Wu et al., 2014). However, the
48 practical application of these anodes is mainly hindered by its shorter service lifetime (Sun et
49 al., 2015). In this sense, studies have been developed in the direction of improving the service
50 life of $\text{Ti/SnO}_2\text{-Sb}$ anodes, and many inputs have been evaluated, such as the addition of

51 dopants (Xu et al., 2012; Sun et al., 2015) or the modification of the calcination temperature
52 (Lei et al., 2018) and heating rate (Da Silva et al., 2018).

53 In recent previous work, Ti/SnO₂-Sb anodes synthesized using CO₂ laser heating were
54 found to be five-fold more stable than conventional anode made by conventional heating in
55 furnaces (Santos et al., 2020). The main advantages of this novel technique of fabrication are
56 the fast heating and cooling rate (Santos et al., 2019), which do not also reduce costs but
57 mainly improves the electrochemical properties of this material, turning it competitive for the
58 oxidation of organic compounds.

59 In this context, phenol appears as a standard reaction to evaluate the performance of
60 novel materials or processes in wastewater treatment, because of the well-known reactivity
61 towards oxidants generated during electrolysis. Moreover, its simple and representative
62 structure makes phenol one of the most significant model pollutants in water research (Ahmed
63 et al., 2010; Villegas et al., 2016; Brillas and Garcia-Segura, 2019; Jun et al., 2019; Ribeiro et
64 al., 2019). It is reported that in using active anodes, treatment of phenol, or phenolic
65 compounds leads to the deposition of adhesive polymeric by-products, which are responsible
66 for the decrease in the electrode activity and, sometimes, in the deactivation of the catalytic
67 surface (Iniesta et al., 2001). Opposite, with non-active electrodes, the complete
68 mineralization can be reached, as there are no heteroatoms in this model compound.

69 In the present work, it is evaluated the performance in the electrochemical oxidation of
70 an improved Ti/SnO₂-Sb anode, using phenol as a model compound to be degraded
71 electrochemically. As explained before, the oxidation mechanisms of this aromatic pollutant
72 are well-known, and there are many papers in the literature reporting electrochemical
73 oxidation of phenol, which are going to be used for comparison purposes. The performance of
74 this novel anode is going to be compared to that of the conventional furnace-made anode.

75 Various conditions were applied, and the mechanisms under which hydroxyl and chlorine
76 radicals attack are compared.

77

78 **2. Experimental section**

79 **2.1 Chemicals**

80 Phenol (99.5 %) from Sigma Aldrich[®], sodium sulfate (99.0%, Vetec[®]), and sodium chloride
81 (99.0%, Neon[®]) were used to compose the electrolytic solutions. The initial pH was adjusted
82 using solutions of 1.0 M H₂SO₄ (95–97%, Emsure[®]) or 0.5 M NaOH (97%, Vetec[®]).
83 Immediately after aliquots were withdrawn, NaHSO₃ (SO₂ ≥ 58.5%, Dinâmica[®]) solution in
84 the same proportion of the chloride was added to quench the oxidants presents in the solution.
85 All solutions were prepared using ultrapure water (Gehaka MS 2000 system).

86

87 **2.2 Preparation of the electrodes**

88 The Ti/SnO₂-Sb anodes were prepared by thermal decomposition of polymeric precursors
89 (also known as the Pechini method) using CO₂ laser heating (GEM-100 L – Coherent). In
90 order to obtain the precursors' solutions, SnCl₂ (99.99%), SbCl₃ (99.99%), anhydrous citric acid
91 (99%), and ethylene glycol (99.8%) were used, all purchased from Sigma-Aldrich[®]. First, the
92 titanium plates were pre-treated, as previously reported (Da Silva et al., 2018). Then, the
93 metallic precursors were dissolved in the citric acid (CA) and ethylene glycol (EG) at 90 °C,
94 according to the molar ratio 10:6:1 (EG/CA/metal molar ratio), where the Sn/Sb molar ratio
95 for the coating preparation was 0.94/0.06. After spreading the obtained precursor solution
96 over both sides of the titanium plates, the thermal treatment was conducted. For the laser
97 heating, the strategy was to increase the power density 0.01 W/mm² reaching a power density
98 of 0.3 W/mm², allowing the temperature reach to 600 °C almost instantaneously, which was

99 kept constant for 15 min and then cooled immediately to room temperature (Santos et al.,
100 2020).

101 For comparison, Ti/SnO₂-Sb anodes were produced using the furnace exclusively,
102 under the same conditions. The loading amount of coating was controlled at ~1.2 mg cm⁻²,
103 which required four brush-pyrolysis stages for both calcination processes. It is essential to
104 point out that for the laser-made anode, the first layer was calcined using the furnace, and the
105 remaining three layers were calcined by laser heating only.

106

107 *2.3 Electrochemical Characterization*

108 Cyclic voltammetry (CV) measurements were obtained from applying 50 mV s⁻¹, varying
109 from 0.0 to 2.0 V. Studies with electrochemical impedance spectroscopy (EIS) were carried
110 out covering the frequency range from 0.1 Hz – 10 kHz with a logarithmic distribution of 10
111 frequencies per decade using an AC sine signal amplitude of 5 mV. Potential applied for EIS
112 was considered as the potential regions of the onset of the oxygen evolution reaction (OER)
113 for each anode. Both characterizations were carried out in supporting electrolyte containing
114 0.1 M Na₂SO₄ in the presence or absence of the phenol (50 mg L⁻¹). The service lifetime tests
115 were performed in the 0.1 M Na₂SO₄ background solution at an applied current density of 200
116 mA cm⁻². The anodes were considered deactivated when the measured potential reached a
117 value of 10.0 V.

118

119 *2.4 Electrolysis*

120

121 The degradations were carried out in a one-compartment electrochemical cell using a Pt plate
122 as the counter electrode. As anodes plates of 10 cm² of Ti/SnO₂-Sb obtained by the novel laser
123 radiation (Santos et al., 2020) and the traditional thermal decomposition using a furnace

124 (Pechini method) were used. A volume of 0.15 L aqueous solution containing phenol was
125 treated. The investigated variables were the concentration of the NaCl (0.0–0.07 M) in the
126 supporting electrolyte (Na₂SO₄ 0.1 M), the cell potential (6–10 V), the pH of the bulk solution
127 (2–10) and the initial concentration of phenol (10–100 mg L⁻¹). The pH values were
128 monitored throughout reaction time (60 min).

129

130 *2.5 Analytical procedures*

131 Samples were collected at given times of reaction and analyzed in an HPLC (Shimadzu 20A
132 LC system with a UV detector). A Phenomenex reversed-phase C18 column was used as the
133 stationary phase (150 mm × 4.6 mm, 5 μm particle size) and a mixture of 70 % acetonitrile
134 and 30 % ultrapure water as mobile phase at a flow rate of 1 mL min⁻¹. The sample injection
135 was 20 μL, and the detection wavelength was 270 nm.

136 The energy consumption (EC, in (kWh (g TOC)⁻¹) was obtained according to the Eq. (1),
137 where E_{cell} is the cell potential (V), I is the current intensity applied (A), t is the electrolysis
138 time (s), V is the volume of treated solution (L), and Δ(TOC) is the variation in the TOC
139 removal (Garcia-Segura and Brillas, 2016).

140

$$141 \quad EC = \frac{E_{cell} \times I \times t}{V \times \Delta(\text{TOC})} \quad (1)$$

142

143 The specific electrical energy (E_{EO}) was used as figure-of-merit for comparison
144 purposes with other advanced oxidation processes, in terms of cost-efficiency. The E_{EO} is
145 defined as the electrical energy (kWh) required to reduce the concentration of pollutants by
146 one order of magnitude (i.e., by 90%) in 1 m³ of water and can be calculated from Eq. (2) for
147 batch operation mode. In this equation, E_{cell} is cell potential (V), I is the average applied
148 current density (A), and t is the electrolysis time (h) (Bolton et al., 2001; Garcia-Segura and

149 Brillas, 2016; Lanzarini-Lopes et al., 2017). This expression can be simplified, assuming first-
 150 order kinetics, according to Eq. (3), because of $\log(C_0/C_f) = 0.4343 k_1 t$, where t (min), k_1 is
 151 the pseudo-first-order constant (min^{-1}). And 38.4×10^{-4} is a conversion factor (1 h / 60 min /
 152 0.4343) (Bolton et al., 2001).

153

$$154 \quad E_{EO} (\text{KW h m}^{-3} \text{ order}^{-1}) = \frac{E_{cell} \times I \times t}{V \times \log(C_0/C_f)} \quad (2)$$

$$155 \quad E_{EO} (\text{KW h m}^{-3} \text{ order}^{-1}) = \frac{38.4 \times 10^{-4} \times E_{cell} \times I}{V \times k_1} \quad (3)$$

156

157 Mineralization current efficiency (MCE) was calculated according to Eq. (4), where n is the
 158 number of electron transfers in the oxidation of phenol ($n=28$), F is the Faraday's constant
 159 ($96.485 \text{ C mol}^{-1}$), V is the solution volume (L), $\Delta(\text{TOC})_{\text{exp}}$ is the experimental solution TOC
 160 decay (mg L^{-1}), n is the number of electrons consumed per phenol molecule (28 mol), m is the
 161 number of carbon atoms of phenol ($m=6$), I is the applied current (A), and t is the electrolysis
 162 time in h, and 4.32×10^7 is a conversion factor for units consistency ($3600 \text{ s h}^{-1} \times 12,000 \text{ mg}$
 163 mol^{-1}) (Lanzarini-Lopes et al., 2017).

164

$$165 \quad \text{MCE} = \frac{n F V (\Delta\text{TOC})}{4.32 \times 10^7 m I t} F V \quad (4)$$

166

167 **3. Results and discussion**

168 *3.1 In situ characterization of the anode*

169 CV and EIS are useful techniques for the investigation of reactions that occurs at the
 170 electrode/solution interface. Here, the Ti/SnO₂-Sb anode produced either using a conventional
 171 furnace, as well as the alternative laser heating, was characterized by CV and EIS in the

172 presence and absence of phenol in the background supporting electrolyte containing Na₂SO₄
173 (Fig. 1).

174 The voltammograms recorded exhibited typical profiles (Fig. 1a,b) in which no change in
175 current occurred in the region between 0.0 and 1.6 V vs. Ag/AgCl, but a current increase
176 related to the oxygen evolution reaction (OER) appears at potentials higher than 1.6 V vs.
177 Ag/AgCl. Moreover, these voltammograms revealed that the presence of phenol increased the
178 anodic charge potentials. On the other hand, results from Nyquist plots (Fig. 1c,d) recorded at
179 the onset potential of the oxygen evolution reaction show the formation of one well-developed
180 semicircle in the medium to low-frequency range (0.1–10⁴ Hz). This behavior agrees with
181 previous studies (Liu et al., 2000; Ding et al., 2010; Santos et al., 2019). The wider semicircle
182 in the presence of phenol shows the increase in the resistivity, which can be explained by the
183 adsorption of the pollutant species onto the anode surface, which is consistent with CV
184 results.

185 Similarly, some authors have reported, for other anode materials, that this increase in the
186 semicircle diameter in EIS spectra may be associated with the presence of 4-chlorophenol or
187 phenol (Karimi-Maleh et al., 2014; Keivani et al., 2017). Also, from EIS results, the diameter
188 of the semicircles for the anode prepared by laser radiation is more than 4 times lower than
189 those observed for the conventional furnace anodes, which indicate a lower charge transfer
190 resistance and suggests a more active surface. Regarding service lifetime tests performed in
191 the background solution (Fig. 1e), the superiority in the stability of the laser-manufactured
192 anode is confirmed by the durability increased 9-fold, at a high applied current density of 200
193 mA cm⁻².

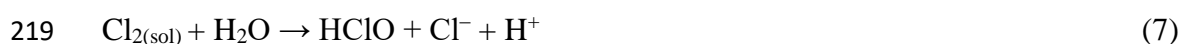
194

195 **3.2 Phenol removal and mineralization**

196 **3.2.1 Influence of the supporting electrolyte concentration**

197 Phenol electrochemical degradation in aqueous solution was performed in different supporting
 198 electrolytes (0.1 M Na₂SO₄ with the addition of NaCl in the range 0.0–0.07 M). The starting
 199 conditions were fixed to be 8 V of potential applied, pH 6, and phenol concentration of 50 mg
 200 L⁻¹. Profiles of phenol decay as a function of the electrolysis time (Fig. 2a) showed that the
 201 pollutant removal in the absence of NaCl (i.e., 0.1 M Na₂SO₄) reached 45.5% after 60 min of
 202 electrolysis. However, in the presence of NaCl, the total removal of the pollutant is achieved
 203 in less than 20 min. This behavior indicates that phenol degradation depends on the nature of
 204 the electrolyte and that it could be occurring by both direct and mediated oxidation. It has
 205 been proposed that hydroxyl radicals formed by water oxidation (H₂O → •OH + H⁺ + e⁻) can
 206 contribute to the oxidation of the organics. On the one hand, as Ti/SnO₂-Sb are classified as
 207 non-active anodes (Rao and Venkatarangaiah, 2014; Wu et al., 2014; Comninellis, 1994), the
 208 hydroxyl radicals (M(•OH)) generated during water oxidation are expected to be the main
 209 oxidizing species produced and can be responsible for the phenol removal in sulfate media.
 210 On the other hand, in the presence of chloride ions, a significant contribution of indirect
 211 oxidation is expected because of the presence of strong chlorine oxidizing species generated
 212 during electrolysis, which explains the faster complete removal of the contaminant. Primarily
 213 chlorine can be disproportionated into hypochlorous acid (HClO), which in turn can be
 214 deprotonated and produce hypochlorite anion (ClO⁻), according to the Equations (5)–(8) (da
 215 Silva et al., 2018; Machado et al., 2018).

216



221

222 The results observed in the present study agree with those from Loloi and coworkers
223 (Loloi et al., 2016), who showed that electrolysis (40 mA cm^{-2}) using a $\text{Ti/SnO}_2\text{-Sb}_2\text{O}_4$ anode
224 with a supporting electrolyte containing chloride ions (0.25 M), the phenol (100 mg L^{-1}) was
225 removed entirely in 1 h, whereas 98.5 % of phenol was removed after 10 h of electrolysis in
226 Na_2SO_4 (0.25 M). In another study, Santos et al. (2011) observed that 90% of phenol was
227 removed after 60 min of electrolysis at 10 mA cm^{-2} from an initial concentration of 100 mg
228 L^{-1} in NaCl 0.34 M as the supporting electrolyte (Santos et al., 2011). Comparing to our data,
229 the $\text{Ti/SnO}_2\text{-Sb}$ anode here studied is much more efficient than the binary oxide ($\text{Ti/SnO}_2\text{-}$
230 Sb_2O_4) reported by Loloi et al. (Loloi et al., 2016) and the $\text{Ti/SnO}_2\text{-Sb}$ reported by Santos et
231 al. (2011) (Santos et al., 2011).

232 From Fig. 2b, it can be pointed out that organic carbon removal is affected by the
233 presence of chlorides. The higher TOC removal is seen for 0.03 M NaCl , and further increase,
234 above this limit, causes a decrease of the organic carbon removal. Similarly, Montanaro and
235 Petrucci (Montanaro and Petrucci, 2009) found a negative effect of sodium chloride addition
236 for values above 0.01 M in the TOC removal of remazol brilliant blue reactive. They showed
237 that when NaCl addition changed from 0.01 to 0.025 M in Na_2SO_4 solution, the time to
238 achieve complete mineralization increased from 240 min to 360 min, while the further
239 increase to 0.05 M NaCl in Na_2SO_4 solution, decreased the TOC abatement to 90% for 360
240 min. This behavior was explained by the different reaction mechanisms promoted in the
241 presence of higher concentrations of chlorides. In this view, it was demonstrated the
242 importance of determining the optimum concentration of chloride (Montanaro and Petrucci,
243 2009). Other authors also suggested an optimum concentration of NaCl for the removal of
244 sulfamethazine (El-Ghenymy et al., 2013), picloram (Coledam et al., 2018) and tebuthiuron
245 (Montes et al., 2017) in electrochemical oxidation based processes, because of the more

246 recalcitrant by-products that are favored at higher concentration of NaCl, which may cause the
247 reduction in the TOC removal.

248 Plots of removal of phenol in electrolytes containing different concentrations of NaCl
249 revealed a linear relationship between reaction time and the natural logarithm of the variation
250 of the pollutant concentration, which means that phenol abatement follows pseudo-first-order
251 kinetics. The rate constant (k) was obtained from the slope of Eq. (9). Where C_0 and C are the
252 initial and final concentrations (in mg L^{-1}) of phenol, respectively, and k (min^{-1}) represents
253 the first-order rate constant, and t is time (min).

254

$$255 \ln \frac{C_0}{C} = k \cdot t \quad (9)$$

256

257 The values of k (min^{-1}) for the phenol removal and percentage of TOC removed
258 according to electrolyte concentration are summarized in Table 1. The energy consumption
259 per mass of TOC removed, as well as the specific electrical energy are critical factors in
260 determining the feasibility of the electrochemical removal of organics from wastewaters. The
261 values of EC and E_{EO} determined for different concentrations of the electrolyte are shown in
262 Table 1. The addition of NaCl reduces the energy consumption gradually reaching a minimum
263 value of $0.55 \text{ kWh (g TOC)}^{-1}$ and $0.67 \text{ kWh m}^{-3} \text{ order}^{-1}$ when 0.07 M NaCl is added. This
264 observation can be explained in terms of the improved conductivity of the solution, as pointed
265 out by Malpass et al. (2012). However, both phenol and TOC removals are faster with the
266 addition of 0.03 M NaCl, and because of this higher rate, this electrolyte was employed in all
267 further experiments. Finally, the highest mineralization current efficiency found was 58.35%,
268 which supports this condition as the more suitable for the subsequent experiments.

269

270 **Table 1.** Observed kinetic constants for phenol removal, energy consumption per unit of TOC
 271 removed, and energy consumption for the electrochemical oxidation of phenol under different
 272 conditions.

Parameter	Phenol Removal $t_{10\min}$ (%)	k (min ⁻¹)	R^2	TOC Removal (%)	EC (kWh(gTOC) ⁻¹)	E_{EO} (kWh m ⁻³ order ⁻¹)	MCE (%)
[NaCl]							
(M)^a							
0	12.75	0.012	0.99	20.9	2.09	47.76	14.34
0.01	84.0	0.208	0.93	22.5	2.32	3.29	18.20
0.03	100	0.592	0.91	52.9	0.80	0.81	58.35
0.05	100	0.555	0.92	45.8	0.75	0.76	24.70
0.07	99.7	0.422	0.85	39.4	0.55	0.67	13.04
pH^b							
2	99.7	0.627	0.86	50.0	2.01	1.60	61.20
10	99.6	0.563	0.969	38.0	1.52	1.77	34.18
E (V)^c							
6	35.6	0.041	0.96	4.00	1.02	1.31	1.00
10	95.8	0.316	0.98	34.0	0.51	0.72	13.2
[Phenol]₀^d							
(mg L⁻¹)							
10	99.4	0.509	0.99	55.0	0.71	0.21	7.90
100	52.9	0.086	0.98	20.0	0.93	5.67	13.2

273 Electrolysis conditions: ^a [Phenol]₀ = 50 mg L⁻¹; pH = 6; E = 8 V; ^b [NaCl] = 0.03 M; E = 8
 274 V; [Phenol]₀ = 50 mg L⁻¹; ^c [NaCl] = 0.03 M; pH = 6; [Phenol]₀ = 50 mg L⁻¹; ^d [NaCl] = 0.03
 275 M; pH = 6; E = 8 V.

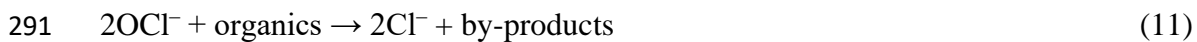
276

277 *a. 2 Influence of initial pH*

278 Investigation of the role of initial pH has been carried out in a range of pH values from acid to
279 alkaline conditions. It is known that the speciation of chlorine depends on the pH, as well as
280 its oxidation capacity. For instance, at acid pH, the hypochlorous acid is the primary species,
281 and it has a higher oxidation capability than the hypochlorite, which is the most important
282 species in the alkaline medium (Wu et al., 2014). Fig. 3a shows that phenol decay is not
283 significantly affected by increasing the pH. Regarding TOC removal (Fig. 3b), the effect is
284 less critical, changing from pH 2 to 6, where similar removals are seen; however, an increase
285 to pH 10 provokes a reduction of 30% in the TOC removal.

286 The acid medium slightly favored the degradation due to the prevalence of the
287 hypochlorous acid (Equation 10), with higher oxidative capacity than the hypochlorite species
288 (Equation 11) (Wu et al., 2014).

289



292

293 As shown in Table 1, the value of k for phenol removal is quite close, varying from
294 0.627 min^{-1} (at pH 2) to 0.563 min^{-1} (pH 10), showing only slight improvement in the
295 sequence: pH 2 > pH 6 > pH 10. It is important to highlight the good applicability of this
296 anode at a wide pH range for the removal of phenol. Regarding the E_{EO} , the lowest value was
297 found at an initial pH of 6 and a slight decrease for pH 2 and 10, which confirms that in the
298 conditions studied, the pH is not of great influence. Therefore, from this point, the pH value
299 was maintained as 6 since no initial adjustment is needed.

300

301 *3.2.3 Influence of the potential applied*

302 Another critical parameter in electrochemical degradation is the potential, which in turn
303 affects the applied current density. As a general trend, at low potential values, only soft
304 oxidation occurs when the electrochemical oxidation is not kinetically limited by mass
305 transport, while an increase in the cell potential increases the removal of pollutants. The
306 higher generation of oxidative species can explain this behavior. However, under mass-
307 transport limitations, the increase in the potential can favor parasitic reactions (i.e., the OER),
308 which must be avoided in wastewater treatment, since they result in a loss in energy and
309 reduces the current efficiency (Martínez-Huitle et al., 2015). In order to evaluate the effect of
310 this parameter, the electrolysis experiments were carried out with applied potential in the
311 range 6 to 10 V (Fig. 3c). When comparing profile decays from 6 to 8 V, the phenol removal
312 increases substantially, resulting in a maximum TOC removal (Fig. 3d). However, an increase
313 up to 10 V prioritizes parallel reactions, probably due to the competition between the reaction
314 of the oxygen evolution reaction and the chlorine formation, leading to a lower TOC removal.

315 The values of the pseudo-first-order rate constants for the removal of phenol at
316 different potential applied are shown in Table 1. The value of k for 8 V is included in the
317 study of the influence of NaCl concentration in the electrolyte. Therefore, the k value for the
318 0.03 M NaCl is the best condition among studied applied potential range (6–10 V) in [NaCl]₀:
319 0.03 M. Also, the potential applied of 8 V (0.03 M NaCl) was determined as optimal for
320 maximum oxidation and TOC removal in the shortest time and with the lowest expenses of
321 energy. Under these conditions, an E_{EO} value of 0.8 kW h m⁻³ order⁻¹ is required to degrade
322 phenol entirely and to remove 52.9% of organic load. This value is much lower when
323 compared to other AOPs to remove phenol from aqueous solutions. Thus, in the O₃-UV-TiO₂
324 (Suzuki et al., 2015), UV-H₂O₂ (Primo et al., 2007), US-H₂O₂-CuO (Drijvers et al., 1999),
325 the E_{EO} values were 28.1, 130.51, 335.92 kW h m⁻³ order⁻¹, respectively.

326

327 3.2.4 Influence of initial concentration of phenol

328 The initial pollutant concentration can affect the performance of the process, so defining the
329 optimal treatable contaminant range is of interest. Initial concentrations in the range of 10–
330 100 mg L^{-1} of phenol were treated at 8 V, in an electrolyte containing 0.03 M NaCl at an
331 initial pH 6. As shown in Fig. 4, the Ti/SnO₂-Sb electrode is efficient at removing phenol at
332 the studied concentrations, with complete phenol removal being observed within 30 min for
333 the highest concentration (100 mg L^{-1}). As expected, and shown in Table 1, the increase in
334 initial phenol concentration produces a decrease in the phenol removal percentage attained
335 after the same electric charge passed and also affects the mineralization (only 20 %
336 mineralization was observed for the highest concentration while for 10 and 50 mg L^{-1} more
337 than 50.0 % of initial concentration is mineralized). This behavior points out that electric
338 charge passes should be adjusted to the organic load of the waste.

339 On the other hand, when comparing specific electrical energy, the values are quite
340 close, ranging from 1.40 to 1.74 kWh m⁻³ order⁻¹, for 10 and 100 mg L^{-1} respectively, which
341 means that the process is limited by mass transfer of the pollutant towards the electrode
342 surface (Tahar and Savall, 1998).

343

344 3.3 Final products

345 At this point, the electrolyses using the conventional anode of Ti/SnO₂-Sb manufactured in a
346 conventional furnace were carried out with the purpose of understanding and compare
347 mechanisms with relation to the laser-made anode. In this scenario, Fig. 5 shows the HPLC
348 chromatograms of the samples in the presence and absence of chlorides for the EO process
349 carried out using the conventional Ti/SnO₂-Sb anode (Fig. 5a,b) and the laser-made anode
350 (Fig. 5c,d). It can be observed the peak related to phenol at a retention time of 5.1 min.
351 Besides, many by-products appearing in the chromatograms were identified based on the

352 literature and using standards of the main by-products. As a result, five of the seven aromatics
353 by-products peaks were identified in the C-18 column, namely hydroquinone, benzoquinone,
354 2- and 4- chlorophenol, and 2,4 dichlorophenol.

355 The identified by-products, structure, and appearance as a function of the time of
356 electrolysis in chloride medium for both anodes are shown in Table SM-1.

357 It is recognized that various oxidative species, such as Cl⁻, hypochlorous
358 acid/hypochlorite (Malpass et al., 2012; Sirés et al., 2014), and •OH radicals (Neto and De
359 Andrade, 2009), are generated during electrolysis in supporting electrolytes containing NaCl
360 and Na₂SO₄, and therefore, different routes may be involved in the degradative process. The
361 reaction mechanism for the electrochemical oxidation of this model organic in Na₂SO₄
362 medium is in agreement with the literature in which the oxidation of phenol on a SnO₂-based
363 anode initially involves •OH radicals as the primary oxidant (Li et al., 2005; Enache and
364 Oliveira-Brett, 2011). Results from HPLC shows that during electrolysis only appears a band
365 with overlapped peaks between 2.8 and 3.3 min retention time (Fig. 5), which corresponding
366 with standard solutions of hydroquinone and benzoquinone, but the presence of other peaks of
367 low intensity may suggest the formation of catechol and resorcinol at lower concentrations
368 (Oliveira et al., 2007). From further analysis, it is worth noting that other aromatic by-
369 products overlapped the absorbance peak of phenol and can be clearly noted an increase in the
370 absorption band around 240 nm (Fig. SM-1), which has been ascribed to the intermediate
371 formation of quinonic compounds. This observation agrees with those from HPLC analysis.
372 Then, first, a reaction mechanism for the EO in Na₂SO₄ media with the Ti/SnO₂-Sb anode
373 used in this work is proposed (Fig. SM-2a) and is in good agreement with the literature in that
374 oxidation reaction involves •OH employing SnO₂-based anodes (Li et al., 2005). In these
375 pathways, first occurs the formation of quinonic by-products (such as hydroquinone and
376 benzoquinone) and in minor proportion probably resorcinol, catechol, followed by the

377 cleavage of the aromatic ring leads to a mixture of carboxylic acids to finally CO₂ (Li et al.,
378 2005; Xu et al., 2012; Loloi et al., 2016).

379 On the other hand, when chloride ions are present, the proposed route (Fig. SM-2b)
380 shows possible mechanisms that involve the addition of Cl[•] along with [•]OH to the phenol
381 molecule. The aromatic ring could suffer attack by active chlorine present in the medium to
382 yield, 2- and 4-chlorophenol, with retention times of 6.3 and 6.7 minutes, respectively, formed
383 mainly as early intermediates, being the 2-chlorophenol formed in higher proportion (Fig.
384 SM-3). These two compounds were followed by the chromatographic area (Fig. SM-3).
385 Further addition of chlorine to both compounds led to the formation of 2,4 dichlorophenol.
386 Furthermore, other peaks of low intensity are speculated to be probably 2,4,6 trichlorophenol
387 at 9.3 minutes of retention time. The chlorinated by-products are totally removed within 60
388 min of treatment in the Na₂SO₄ 0.1 M and with the addition of 0.03 M of NaCl in the
389 supporting electrolyte. On the contrary, for the conventional anode, the removal of phenol is
390 slower ($k = 0.0973$; $R^2:0.93$) (Fig. SM-4), and due to this, the chlorinated by-products are not
391 entirely removed after 60 min of electrolysis.

392 Also, further analysis from UV/Vis spectra of the samples treated using the laser-made
393 Ti/SnO₂-Sb anode suggests that aromatic compounds are entirely removed. Since no band can
394 be detected after 60 min of reaction (Fig. SM-2b), the remaining peaks at around 3 minutes
395 can be related to carboxylic acid formed that were observed to appear at this retention time
396 (here we remind that at the end of the treatment, in the UV/Vis spectra, the peaks
397 corresponding to quinonic compounds are completely decreased) (Fig. SM-2b). Since this
398 optimized condition presented more than 50 % of TOC removed, this can be easily correlated
399 with carboxylic acids formed. Few authors have proposed the degradation of phenol in the
400 NaCl medium for non-active anodes. For example, a recent study by Zhang et al., (2016)
401 reported the role of the concentration of chlorides in the removal of 50 mg L⁻¹ of phenol in a

402 single reactor in batch mode using BDD anodes. They also found there is no apparent
403 improvement in increasing the NaCl concentration (above 0.05 M NaCl) (Zhang et al., 2016).

404

405 *3.4 Comparison of the EO between laser-made Ti/SnO₂-Sb and the literature*

406 Plenty of studies have employed different electrode materials for phenol removal, as
407 previously stated, due to relevance as a model pollutant, structure, and potential hazardous
408 effect (Xu et al., 2012; Sun et al., 2015). In the view to have an in-depth comparison of our
409 data with the literature, here we provide a review on the performance of different SnO₂-based
410 anodes (doped or not) prepared by different techniques that were reported until now in terms
411 of better results obtained towards the removal of phenol (Table 1).

412 The study of electrochemical oxidation to remove phenolic compounds started in the
413 seventies when Nilson et al. (1973) (Nilsson et al., 1973), Mieluch et al. (1975) (Mieluch et
414 al., 1975), and Dabrowski et al. (1976) (Dabrowski et al., 1976) tried this technology for the
415 treatment of wastewaters. Later, the use of electrochemical oxidation for the destruction of
416 phenol in a pilot plant scale was reported in the eighties by De Sucre and Watkinson (De
417 Sucre and Watkinson, 1981), Chettiar and Watkinson (Chettiar and Watkinson, 1983), and
418 Sharifan and Kirk (Sharifian and Kirk, 1986). They used synthetic wastewater solutions
419 containing phenol. Low reaction rates and low efficiencies were the main drawbacks for
420 commercial employment of electrochemical oxidation (the percentages of phenol removed
421 ranged in 53–70%, depending on the operational conditions). One reason for the low reaction
422 rate found was the electrode fouling by some organic polymeric compounds. Phenol is well
423 known for its ability to foul electrodes since it may form polymerization products during
424 electrochemical oxidation (Gattrell and Kirk, 1990; Panizza et al., 2002; Yang et al., 2013).

425 In the nineties, Kotz et al. (1991) (Kötz et al., 1991) and Stucki et al. (1991) (Stucki et
426 al., 1991) in sequenced papers have proposed the use of SnO₂ anode doped with Sb as an

427 alternative candidate for the wastewater treatment. The rate of phenol removal was about 5
428 times higher for Ti/SnO₂-Sb than the Pt or PbO₂ anode.

429 After, Comninellis and Pulgarin (1993) used phenol oxidation as a model reaction for
430 the abatement of organics on Ti/SnO₂-Sb anodes (Comninellis and Pulgarin, 1993). A 90%
431 removal of 2000 mg L⁻¹ of phenol was obtained after 6.25 h at 50 mA cm⁻². In 1994,
432 Comninellis (1994) proposed the mechanisms for the electrochemical oxidation (or
433 combustion) of organics using different anode materials (Pt, Ti/IrO₂, Ti/SnO₂-Sb), where
434 phenol was used as a model pollutant: while SnO₂-Sb anode favored combustion of pollutant,
435 the IrO₂, and Pt anodes favored selective oxidation (Comninellis, 1994). Then, Comninellis
436 and Nerini (1995) studied the oxidation of phenol with Ti/SnO₂-Sb and Ti/IrO₂ anodes in the
437 presence of 0.085 M NaCl. They found a key role of the electrogenerated ClO⁻ in the
438 oxidation of organics close to the anode or into the bulk solution. Phenol was removed after 8
439 h using both anodes regardless of the NaCl concentration. When the Ti/IrO₂ is used the
440 primary oxidation mechanism is mediated by the ClO⁻, and when the Ti/SnO₂-Sb anode is
441 used the attack by an additional amount of the hydroxyl radicals remained more critical, and
442 thus the rate of TOC removal at this anode was much higher than that of Ti/IrO₂ (Comninellis
443 and Nerini, 1995).

444 Li and coworkers reported similar results for the oxidation of phenol at Ti/SnO₂-Sb,
445 Ti/RuO₂, and Pt anodes in 0.25 M Na₂SO₄. The Ti/SnO₂-Sb showed better performance
446 removing phenol after 5 h at the Ti/SnO₂-Sb, which was attributed to the higher generation of
447 hydroxyl radicals. The primary intermediates identified for this anode were hydroquinone and
448 benzoquinone that were further converted into carboxylic acids (Li et al., 2005).

449 In recent years, doping with another element has been reported to improve the
450 performance of the SnO₂-Sb anode. For example, Yang et al. (2012) examined the doping
451 effects of metals on SnO₂-Sb anodes for the removal of phenol. The authors found an

452 enhancement by doping with Ni by a factor up to 14, in terms of phenol degradation at around
453 22.2 mA cm⁻² in 0.1 M Na₂SO₄ (Yang et al., 2012). Regarding SnO₂-Sb doped with
454 molybdenum (Mo), Lian et al. (2015) reported an improvement in the electrocatalytic activity
455 of the anodes in the electrochemical oxidation of phenol. The insertion of 1% of Mo presented
456 a more compact structure and longer service lifetime (36.6% higher than the Ti/SnO₂-Sb).
457 Moreover, higher electrocatalytic activity for removal of phenol (100 mg L⁻¹) in 0.25 M
458 Na₂SO₄ was observed with the use of the Ti/SnO₂-Sb-Mo(1%). Electrolysis performed at 10
459 mA cm⁻² for 3.5 h resulted in 99.6% of removal of phenol and removal of organic load in
460 82.67% de TOC (Liang et al., 2015). Sun et al. (2015), showed that Ti/SnO₂-Sb doped with
461 Ni-Nd could remove 100 % of phenol after 2 h, while for the Ti/SnO₂-Sb anode, 4 h was
462 required (Sun et al., 2015). Berenguer et al. (2016) studied the activity of the Ti/SnO₂-Sb_(13-x)-
463 Pt-Ru_(x) ($x = 0, 3.25, \text{ and } 9.75\%$) toward phenol oxidation in alkaline medium and found that
464 the Ti/SnO₂-Sb-Pt anode presented improved catalytic activity but low stability. The insertion
465 of low quantities of Ru (3.25–9.75%) improved the stability, but decreased the electroactivity:
466 at best conditions, about 85% removal efficiency is attained at 100 mA cm⁻² and 24 h of
467 treatment for the Ti/SnO₂-Sb_(9.75)-Pt-Ru_(3.25). However, the authors have considered
468 consumption and stability and stated that the cost-effectiveness of this anode makes it suitable
469 for phenol removal in alkaline media (Sun et al., 2015; Berenguer et al., 2016).

470 Regarding active anodes, a comparison is also included in Table 2. Compared to the
471 non-active anode here produced, none of the active anodes was capable of removing the
472 pollutant in less than 60 min, even in the presence of chloride ions. It means that the anode
473 proposed in this work is much better not only as compared with non-active anodes but also of
474 active anodes. For example, Santos et al. (2010) found that after 30 min of electrolysis at 10
475 mA cm⁻², 100 mg L⁻¹ of phenol in 20 g L⁻¹ of NaCl, was almost fully removed using Ti/RuO₂
476 anode (Santos et al., 2010). Another study showed that mixed-metal oxides of Ti/SnO₂–

477 RuO₂-IrO₂, Ta₂O₅-IrO₂, and RhO₂-IrO₂ were successfully applied to removal of phenol (47
 478 mg L⁻¹) up to 99–99.3 % after 8 h of electrolysis in the electrolyte containing 0.010 g L⁻¹ KCl
 479 (Makgae et al., 2008).

480

481 **Table 2.** Comparison of the performance of SnO₂-Sb based anodes for the oxidation of phenol
 482 in aqueous medium under the best operational conditions.

Preparation method	Experimental method	Best phenol removal	Reference
Non-active anodes			
Ti/SnO ₂ -Sb — 600°C Pechini method (laser heating)	t = 1 h P _{cell} = 8V C ₀ = 50 mg L ⁻¹ v = 200 mL Electrolyte = 0.1 M Na ₂ SO ₄ + 30 M NaCl Anodic area = 10 cm ²	100% decay after 10 min 52.9% TOC decay K = 0.592 (R ² :)	This work
Ti/SnO ₂ -Sb — 600°C Conventional Pechini method	t = 1 h P _{cell} = 8V C ₀ = 50 mg L ⁻¹ v = 200 mL Electrolyte = 0.1 M Na ₂ SO ₄ + 0.03 M NaCl Anodic area = 10 cm ²	100% decay after 60 min 8.8% TOC decay k = 0.0973 (R ² :0.93)	This work
Ti/SnO ₂ -Sb-Ni-Nd — 550°C sol-gel method	t = 4 h j = 10 mA cm ⁻² C ₀ = 50 mg L ⁻¹ v = 60 mL Electrolyte = 0.05 M Na ₂ SO ₄ Anodic area = 8 cm ²	100% decay before 2 h 90.8% TOC decay after 4 h	(Sun et al., 2015)
SnO ₂ -Sb — 550°C Pechini Method	t = 2.5 h j = 30 mA cm ⁻² C ₀ = 500 mg L ⁻¹ v = 100 mL Electrolyte = 0.1 M Na ₂ SO ₄	60.2% COD 83.6% decay k = 0.018 min ⁻¹	(Xu et al., 2012)
SnO ₂ -Sb — 600 °C Pechini method	t = 60 min j = 10 mA cm ⁻² C ₀ = 100 mg L ⁻¹ v = 200 mL Electrolyte = 0.34 M NaCl Anodic area = 27 cm ²	90% decay	(Santos et al., 2011)
Ti/SnO ₂ -Sb — 400 °C electrodeposition	t = 50 min j = 20 mA cm ⁻² / P _{cell} = 4.6 V C ₀ = 490 mg L ⁻¹ v = 80 mL Electrolyte = 0.25 M Na ₂ SO ₄	100% TOC decay after 16 h 100% decay after 5h	(Li et al., 2005)

	Anodic area = 6 cm ²		
Ti/SnO ₂ -Sb-Mo — 600 °C dip-coating	t = 3.5 h j = 10 mA cm ⁻² C ₀ = 100 mg L ⁻¹ v = 400 mL Electrolyte = 0.25 M Na ₂ SO ₄ Anodic area = 2 cm ²	99.62% decay 82.67% TOC decay	(Liang et al., 2015)
SnO ₂ -Sb-Ni	t = 0.02 L j = 22.2 mA cm ⁻² C ₀ = 7.5 g L ⁻¹ v = 200 mL Electrolyte = 0.1 M Na ₂ SO ₄ Anodic area = 4.5 cm ⁻²	100% decay after 20 min k = 0.03 min ⁻¹	(Yang et al., 2012)
Ti/SnO ₂ -Sb ₂ O ₄ — 450°C electrodeposition and dip- coating	t = 3 h P _{cell} = 2 V C ₀ = 20 mg L ⁻¹ v = 100 mL Electrolyte = not informed Anodic area = 7 cm ² 250 W – high pressure mercury lamp (λ = 365 nm)	85% TOC removal after 3 h 100% decay after 2 h	(Yan et al., 2009)
Ti/ SnO ₂ -Sb — 600°C ultrasonic spray pyrolysis	t = not informed j = 10 mA cm ⁻² COD ₀ = 1174 mg L ⁻¹ v = not informed Electrolyte = 1500 mg L ⁻¹ Na ₂ SO ₄ Anodic area = 7.7 cm ⁻²	97% DOC removal after a charge loading of 7 Ah L ⁻¹	(Yao, 2011)
Ti/SnO ₂ -Sb ₂ O ₃ -Nb ₂ O ₅ /PbO ₂ — 480°C thermal decomposition/electrochemical deposition	t = 2 h j = 20 mA cm ⁻² C ₀ = 500 mg L ⁻¹ v = 50 mL Electrolyte = 21.3 g L ⁻¹ NaCl Anodic area = 5.5 cm ²	97.2% decay	(Yang et al., 2009)
Active anodes			
Ti/RuO ₂ - commercial [®]	t = 360 min j = 10 mA cm ⁻² C ₀ = 100 mg L ⁻¹ v = 0.25 L Electrolyte = 20 g L ⁻¹ NaCl Anodic area = 27 cm ²	99.6% decay	(Santos et al., 2010)
Ti/IrO ₂ -Ta ₂ O ₅ or Ti/SnO ₂ - RuO ₂ -IrO ₂ or Ti/RhO ₂ -IrO ₂ Sol-gel method	t = 8 h E = 1.5 V C ₀ = 47 mg L ⁻¹ v = 50 mL Electrolyte = 0.01 g L ⁻¹ KCl Anodic area = 1 cm ²	99 – 99.3% decay	(Makgae et al., 2008)
Ti/RuO ₂ - commercial [®]	t = 180 min j = 119 mA cm ⁻² C ₀ = 100 mg L ⁻¹ v = 1 L	100% COD decay 100% decay	(Fajardo et al., 2017a)

	pH ₀ = 3.4 Electrolyte = 10 mg L ⁻¹ NaCl Anodic area = 21.1 cm ²		
70TiO ₂ /30RuO ₂ - thermal deposition	t = 90 min j = 20 mA cm ⁻² C ₀ = 50 mg L ⁻¹ v = 300 mL pH ₀ = 7 Electrolyte = 0.1 M Na ₂ SO ₄ Anodic area = 100 cm ² UV lamp = 125 W	85% decay and 70% TOC decay after 90 min	(Pelegri ni et al., 2001)
Ti/IrO ₂ commercial [®]	t = 180 min j = 119 mA cm ⁻² C ₀ = 100 mg L ⁻¹ v = 1000 mL pH = 3.4 Electrolyte = 10 mg L ⁻¹ NaCl Anodic area = 21.1 cm ²	100% decay phenolic content 84.8% COD decay	(Fajardo et al., 2017b)
70TiO ₂ /30RuO ₂ commercial [®]	t = 300 min j = 100 mA cm ⁻² C ₀ = 100 mg L ⁻¹ v = 500 mL pH = 4 flow rate = 120 L h ⁻¹ Electrolyte = 0.5 M of Na ₂ SO ₄ and H ₂ SO ₄ Anodic area = 21.6 cm ²	90% decay after 2 h	(Pelegri ni et al., 2002)
Ti/Ni _x O _y -RuO ₂ -SnO ₂ -Sb ₂ O ₅ - thermal decomposition	t = 60 min j = 70 mA cm ⁻² C ₀ = 300 mg L ⁻¹ v = 1000 mL pH = 2 Electrolyte = 4 g L ⁻¹ NaCl Anodic area = about 40 cm ²	73.6% COD decay	(Saxena and Ruparelia, 2018)

483

484 Finally, from the above comparison, it can be highlighted that the anode produced in
485 this research is very promising, and it has confirmed an outstanding performance, previously
486 suggested in our previous paper (Santos et al., 2020). The proposed mechanisms of oxidation
487 in different conditions described here will be useful to compare the performance of EAOP
488 through figures of merit in order to evaluate the operating performance as well as associated
489 energy costs.

490

491 **Conclusions**

492 From this work, the following conclusions can be drawn:

- 493 - The Ti/SnO₂-Sb laser-made anode presented improved electrocatalytic properties and
494 easier charge transfer in the tested electrolytes, comparing favorably with conventional
495 electrodes of the same composition and allowing better treatment results than other
496 competing anode materials.
- 497 - The best conditions for the electrochemical oxidation of phenol using the novel Ti/SnO₂-
498 Sb anode were achieved in this work using 0.030 M NaCl, 8 V of applied potential, and
499 pH 6. These conditions led to the highest percentage of TOC removal, which was
500 associated with relatively low energy consumption. Compared with a conventional
501 furnace-made anode, the kinetics for phenol removal was 6.1 faster.
- 502 - The increase of applied potential to 10 V does not improve degradation efficiency. It is
503 explained in terms of the promotion of side reactions favored at the anode surface. Also, a
504 further increase in NaCl in the electrolyte increases (> 0.03 M) does not alter the pollutant
505 removal kinetics significantly but reduces the TOC removal, which was related to the
506 accumulation of more refractory organochlorinated.
- 507 - Chlorinated by-products were identified, and cleavage of the aromatic ring by hydroxyl
508 and/or chlorine radicals led to the formation of carboxylic acids and complete removal of
509 aromatics under the electrolytic conditions employed was observed only for the laser-
510 made anode.
- 511 - The results presented here demonstrated the efficiency of the electrochemical oxidation
512 using a laser-made Ti/SnO₂-Sb for wastewater treatment, pointing out its promising
513 features for future applications.

514

515 **Acknowledgments**

516 The authors acknowledge the financial support from the Brazilian agencies (*Conselho*
517 *Nacional de Desenvolvimento Científico e Tecnológico* – CNPq grants 304419/2015-0,

518 305438/2018-2, 160115/2019-1 and 311856/2019-5), *Coordenação de Aperfeiçoamento de*
519 *Pessoal de Nível Superior – CAPES* (88882.365552. /2018-01 and 88881.187890/2018-01)
520 and FAPITEC/SE (019.203.00926/2016-4) and the *Agencia Estatal de Investigación* and
521 European Union through project CTM2016-76197-R (AEI/FEDER, UE). We also thank Prof.
522 Dr. Ronaldo Santos da Silva from the Federal University of Sergipe for the equipment for the
523 CO₂ laser synthesis.

524

525 **References**

- 526 Ahmed, S., Rasul, M., Martens, W.N., Brown, R., Hashib, M., 2010. Heterogeneous photocatalytic
527 degradation of phenols in wastewater: a review on current status and developments. *Desalination*
528 261, 3–18.
- 529 Berenguer, R., Sieben, J.M., Quijada, C., Morallón, E., 2016. Electrocatalytic degradation of phenol
530 on Pt-and Ru-doped Ti/SnO₂-Sb anodes in an alkaline medium. *Appl. Catal. B: Environ.* 199,
531 394–404.
- 532 Bolton, J.R., Bircher, K.G., Tumas, W., Tolman, C.A., 2001. Figures-of-merit for the technical
533 development and application of advanced oxidation technologies for both electric-and solar-
534 driven systems (IUPAC Technical Report). *Pure Appl. Chem.* 73, 627–637.
- 535 Brillas, E., Garcia-Segura, S., 2019. Benchmarking recent advances and innovative technology
536 approaches of Fenton, photo-Fenton, electro-Fenton, and related processes: A review on the
537 relevance of phenol as model molecule. *Sep. Purif. Technol.* 237, 116337.
- 538 Chettiar, M., Watkinson, A., 1983. Anodic oxidation of phenolics found in coal conversion effluents.
539 *Can. J. Chem. Eng.* 61, 568-574.
- 540 Coledam, D.A., Sánchez-Montes, I., Silva, B.F., Aquino, J.M., 2018. On the performance of
541 HOCl/Fe²⁺, HOCl/Fe²⁺/UVA, and HOCl/UVC processes using in situ electrogenerated active
542 chlorine to mineralize the herbicide picloram. *Appl. Catal. B: Environ.* 227, 170-177.
- 543 Comninellis, C., 1994. Electrocatalysis in the electrochemical conversion/combustion of organic
544 pollutants for waste water treatment. *Electrochim. Acta* 39, 1857-1862.
- 545 Comninellis, C., Nerini, A., 1995. Anodic oxidation of phenol in the presence of NaCl for wastewater
546 treatment. *J. Appl. Electrochem.* 25, 23-28.
- 547 Comninellis, C., Pulgarin, C., 1993. Electrochemical oxidation of phenol for wastewater treatment
548 using SnO₂, anodes. *J. Appl. Electrochem.* 23, 108-112.
- 549 Da Silva, L.M., Santos, G.O.S., de Salles Pupo, M.M., Eguiluz, K.I.B., Salazar-Banda, G.R., 2018.
550 Influence of heating rate on the physical and electrochemical properties of mixed metal oxides

551 anodes synthesized by thermal decomposition method applying an ionic liquid. *J. Electroanal.*
552 *Chem.* 813, 127-133.

553 Dabrowski, A., Mieluch, J., Sadkowski, A., Wild, J., Zoltowski, P., 1976. Pilot-plant study of
554 electrochemical phenol-waste purification. *Przemysl Chemiczny*, 54, 653-655.

555 De Sucre, V.S., Watkinson, A., 1981. Anodic oxidation of phenol for waste water treatment. *Can. J.*
556 *Chem. Eng.* 59, 52-59.

557 Ding, H.-Y., Feng, Y.-J., Lu, J.-W., 2010. Study on the service life and deactivation mechanism of
558 Ti/SnO₂-Sb electrode by physical and electrochemical methods. *Russ. J. Electrochem.* 46, 72-76.

559 Drijvers, D., Van Langenhove, H., Beckers, M., 1999. Decomposition of phenol and trichloroethylene
560 by the ultrasound/H₂O₂/CuO process. *Water Res.* 33, 1187-1194.

561 El-Ghenemy, A., Cabot, P.L., Centellas, F., Garrido, J.A., Rodríguez, R.M., Arias, C., Brillas, E.,
562 2013. Electrochemical incineration of the antimicrobial sulfamethazine at a boron-doped diamond
563 anode. *Electrochim. Acta* 90, 254-264.

564 Enache, T.A., Oliveira-Brett, A.M., 2011. Phenol and para-substituted phenols electrochemical
565 oxidation pathways. *J. Electroanal. Chem.* 655, 9-16.

566 Fajardo, A.S., Seca, H.F., Martins, R.C., Corceiro, V.N., Freitas, I.F., Quinta-Ferreira, M.E., Quinta-
567 Ferreira, R., 2017a. Electrochemical oxidation of phenolic wastewaters using a batch-stirred
568 reactor with NaCl electrolyte and Ti/RuO₂ anodes. *J. Electroanal. Chem.* 785, 180-189.

569 Fajardo, A.S., Seca, H.F., Martins, R.C., Corceiro, V.N., Vieira, J.P., Quinta-Ferreira, M.E., Quinta-
570 Ferreira, R.M., 2017b. Phenolic wastewaters depuration by electrochemical oxidation process
571 using Ti/IrO₂ anodes. *Environ. Sci. Pollut. R.* 24, 7521-7533.

572 Garcia-Segura, S., Brillas, E., 2016. Combustion of textile monoazo, diazo and triazo dyes by solar
573 photoelectro-Fenton: decolorization, kinetics and degradation routes. *Appl. Catal. B: Environ.*
574 181, 681-691.

575 Gattrell, M., Kirk, D., 1990. The electrochemical oxidation of aqueous phenol at a glassy carbon
576 electrode. *Can. J. Chem. Eng.* 68, 997-1003.

577 Iniesta, J., Michaud, P., Panizza, M., Cerisola, G., Aldaz, A., Comninellis, C., 2001. Electrochemical
578 oxidation of phenol at boron-doped diamond electrode. *Electrochim. Acta* 46, 3573-3578.

579 Jun, L.Y., Yon, L.S., Mubarak, N., Bing, C.H., Pan, S., Danquah, M.K., Abdullah, E., Khalid, M.,
580 2019. An Overview of Immobilized Enzyme Technologies for Dye, Phenolic Removal from
581 Wastewater. *J. Environ. Chem. Eng.* 7, 102961.

582 Karimi-Maleh, H., Moazampour, M., Ensafi, A.A., Mallakpour, S., Hatami, M., 2014. An
583 electrochemical nanocomposite modified carbon paste electrode as a sensor for simultaneous
584 determination of hydrazine and phenol in water and wastewater samples. *Environ. Sci. Pollut. R.*
585 21, 5879-5888.

586 Keivani, Z., Shabani-Nooshabadi, M., Karimi-Maleh, H., 2017. An electrochemical strategy to
587 determine thiosulfate, 4-chlorophenol and nitrite as three important pollutants in water samples
588 via a nanostructure modified sensor. *J. Colloid Interf. Sci.* 507, 11-17.

589 Kötzt, R., Stucki, S., Carcer, B., 1991. Electrochemical waste water treatment using high overvoltage
590 anodes. Part I: Physical and electrochemical properties of SnO₂ anodes. *J. Appl. Electrochem.* 21,
591 14-20.

592 Lanzarini-Lopes, M., Garcia-Segura, S., Hristovski, K., Westerhoff, P., 2017. Electrical energy per
593 order and current efficiency for electrochemical oxidation of p-chlorobenzoic acid with boron-
594 doped diamond anode. *Chemosphere* 188, 304-311.

595 Lei, X., Li, L., Chen, Y., Hu, Y., 2018. Effect of calcination temperature on the properties of Ti/SnO₂-
596 Sb anode and its performance in Ni-EDTA electrochemical degradation. *Environ. Sci. Pollut. R.*
597 25, 11683-11693.

598 Li, X.-y., Cui, Y.-h., Feng, Y.-j., Xie, Z.-m., Gu, J.-D., 2005. Reaction pathways and mechanisms of
599 the electrochemical degradation of phenol on different electrodes. *Water Res.* 39, 1972-1981.

600 Liang, J., Geng, C., Li, D., Cui, L., Wang, X., 2015. Preparation and degradation phenol
601 characterization of Ti/SnO₂-Sb-Mo electrode doped with different contents of molybdenum. *J.*
602 *Mater. Sci. Technol.* 31, 473-478.

603 Liu, H., Cheng, S., Wu, M., Wu, H., Zhang, J., Li, W., Cao, C., 2000. Photoelectrocatalytic
604 degradation of sulfosalicylic acid and its electrochemical impedance spectroscopy investigation.
605 *J. Phys. Chem. A* 104, 7016-7020.

606 Loloi, M., Rezaee, A., Aliofkhaeaei, M., Rouhaghdam, A.S., 2016. Electrocatalytic oxidation of
607 phenol from wastewater using Ti/SnO₂-Sb₂O₄ electrode: chemical reaction pathway study.
608 *Environ. Sci. Pollut. R.* 23, 19735-19743.

609 Machado, C.F., Gomes, M.A., Silva, R.S., Salazar-Banda, G.R., Eguiluz, K.I.B., 2018. Time and
610 calcination temperature influence on the electrocatalytic efficiency of Ti/SnO₂:Sb (5%), Gd (2%)
611 electrodes towards the electrochemical oxidation of naphthalene. *J. Electroanal. Chem.* 816, 232-
612 241.

613 Makgae, M., Klink, M., Crouch, A., 2008. Performance of sol-gel Titanium Mixed Metal Oxide
614 electrodes for electro-catalytic oxidation of phenol. *Appl. Catal. B: Environ.* 84, 659-666.

615 Malpass, G.R., Miwa, D.W., Santos, R.L., Vieira, E.M., Motheo, A.J., 2012. Unexpected toxicity
616 decrease during photoelectrochemical degradation of atrazine with NaCl. *Environ. Chem. Lett.*
617 10, 177-182.

618 Marselli, B., Garcia-Gomez, J., Michaud, P.-A., Rodrigo, M., Comninellis, C., 2003. Electrogeneration
619 of hydroxyl radicals on boron-doped diamond electrodes. *J. Electrochem. Soc.* 150, D79-D83.

620 Martínez-Huitle, C.A., Rodrigo, M.A., Sirés, I., Scialdone, O., 2015. Single and coupled
621 electrochemical processes and reactors for the abatement of organic water pollutants: a critical
622 review. *Chem. Rev.* 115, 13362-13407.

623 Mieluch, J., Sadkowski, A., Wild, J., Zoltowski, P., 1975. Electrochemical oxidation of phenol
624 compounds in aqueous-solutions. *Przem. Chem.* 54, 513-516.

625 Montanaro, D., Petrucci, E., 2009. Electrochemical treatment of Remazol Brilliant Blue on a boron-
626 doped diamond electrode. *Chem. Eng. J.* 153, 138-144.

627 Montes, I.J., Silva, B.F., Aquino, J.M., 2017. On the performance of a hybrid process to mineralize the
628 herbicide tebuthiuron using a DSA[®] anode and UVC light: a mechanistic study. *Appl. Catal. B:
629 Environ.* 200, 237-245.

630 Moreira, F.C., Boaventura, R.A., Brillas, E., Vilar, V.J., 2017. Electrochemical advanced oxidation
631 processes: a review on their application to synthetic and real wastewaters. *Appl. Catal. B:
632 Environ.* 202, 217-261.

633 Neto, S.A., De Andrade, A.R., 2009. Electrooxidation of glyphosate herbicide at different DSA[®]
634 compositions: pH, concentration and supporting electrolyte effect. *Electrochim. Acta* 54, 2039-
635 2045.

636 Nilsson, A., Ronlán, A., Parker, V.D., 1973. Anodic oxidation of phenolic compounds. Part III.
637 Anodic hydroxylation of phenols. A simple general synthesis of 4-alkyl-4-hydroxycyclo-hexa-2,
638 5-dienones from 4-alkylphenols. *J. Chem. Soc. Perkin.* 1 2337-2345.

639 Oliveira, R.T., Salazar-Banda, G.R., Santos, M.C., Calegario, M.L., Miwa, D.W., Machado, S.A.,
640 Avaca, L.A., 2007. Electrochemical oxidation of benzene on boron-doped diamond electrodes.
641 *Chemosphere* 66, 2152-2158.

642 Panizza, M., Michaud, P.-A., Iniesta, J., Comninellis, C., Cerisola, G., 2002. Electrochemical
643 oxidation of phenol at boron-doped diamond electrode. Application to electro-organic synthesis
644 and wastewater treatment. *Ann. Chim.* 92, 995-1006.

645 Pelegrini, R., Freire, R., Duran, N., Bertazzoli, R., 2001. Photoassisted electrochemical degradation of
646 organic pollutants on a DSA type oxide electrode: process test for a phenol synthetic solution and
647 its application for the E1 bleach kraft mill effluent. *Environ. Sci. Technol.* 35, 2849-2853.

648 Pelegrino, R.L., Di Iglia, R.A., Sanches, C.G., Avaca, L.A., Bertazzoli, R., 2002. Comparative study
649 of commercial oxide electrodes performance in electrochemical degradation of organics in
650 aqueous solutions. *J. Braz. Chem. Soc.* 13, 60-65.

651 Primo, O., Rivero, M.J., Ortiz, I., Irabien, A., 2007. Mathematical modelling of phenol
652 photooxidation: Kinetics of the process toxicity. *Chem. Eng. J.* 134, 23-28.

653 Radjenovic, J., Sedlak, D.L., 2015. Challenges and opportunities for electrochemical processes as
654 next-generation technologies for the treatment of contaminated water. *Environ. Sci. Technol.* 49,
655 11292-11302.

656 Rao, A.N.S., Venkatarangiah, V.T., 2014. Metal oxide-coated anodes in wastewater treatment.
657 *Environ. Sci. Pollut. R.* 21, 3197-3217.

658 Ribeiro, A.R., Moreira, N.F., Puma, G.L., Silva, A.M., 2019. Impact of water matrix on the removal of
659 micropollutants by advanced oxidation technologies. *Chem. Eng. J.* 363, 155-173.

660 Santos, G.O.S., Vasconcelos, V.M., da Silva, R.S., Rodrigo, M.A., Eguiluz, K.I.B., Salazar-Banda,
661 G.R., 2020. New laser-based method for the synthesis of stable and active Ti/SnO₂-Sb anodes.
662 *Electrochim. Acta*, **332**, 135478.

663 Santos, G.O.S., Silva, L.R.A., Alves, Y.G.S., Silva, R.S., Eguiluz, K.I.B. Salazar-Banda G.R., 2019
664 Enhanced stability and electrocatalytic properties of Ti/Ru_xIr_{1-x}O₂ anodes produced by a new
665 laser process, *Chem. Eng. J.* **355**, 439-447.

666 Santos, I., Afonso, J., Dutra, A., 2010. Behavior of a Ti/RuO₂ anode in concentrated chloride medium
667 for phenol and their chlorinated intermediates electrooxidation. *Sep. Purif. Technol.* **76**, 151-157.

668 Santos, I.D., Gabriel, S.B., Afonso, J.C., Dutra, A.J.B., 2011. Preparation and characterization of
669 Ti/SnO₂-Sb electrode by Pechini's method for phenol oxidation. *Mat. Res.* **14**, 408-416.

670 Saxena, P., Ruparelia, J., 2018. Electrochemical degradation of Simulated Phenolic Wastewater using
671 Ti/Ni_xO_y-RuO₂-SnO₂-Sb₂O₅ anode. *Int. J. Appl. Environ. Sci.* **13**, 811-821.

672 Sharifian, H., Kirk, D., 1986. Electrochemical oxidation of phenol. *J. Electrochem. Soc.* **133**, 921.

673 Sirés, I., Brillas, E., Oturan, M.A., Rodrigo, M.A., Panizza, M., 2014. Electrochemical advanced
674 oxidation processes: today and tomorrow. A review. *Environ. Sci. Pollut. R.* **21**, 8336-8367.

675 Stucki, S., Kötzt, R., Carcer, B., Suter, W., 1991. Electrochemical waste water treatment using high
676 overvoltage anodes Part II: Anode performance and applications. *J. Appl. Electrochem.* **21**, 99-
677 104.

678 Sun, Z., Zhang, H., Wei, X., Du, R., Hu, X., 2015. Fabrication and electrochemical properties of a
679 SnO₂-Sb anode doped with Ni-Nd for phenol oxidation. *J. Electrochem. Soc.* **162**, H590-H596.

680 Suzuki, H., Araki, S., Yamamoto, H., 2015. Evaluation of advanced oxidation processes (AOP) using
681 O₃, UV, and TiO₂ for the degradation of phenol in water. *J. Water Process Eng.* **7**, 54-60.

682 Tahar, N.B., Savall, A., 1998. Mechanistic aspects of phenol electrochemical degradation by oxidation
683 on a Ta/PbO₂ anode. *J. Electrochem. Soc.* **145**, 3427-3434.

684 Villegas, L.G.C., Mashhadi, N., Chen, M., Mukherjee, D., Taylor, K.E., Biswas, N., 2016. A short
685 review of techniques for phenol removal from wastewater. *Curr. Pollut. Rep.* **2**, 157-167.

686 Wu, W., Huang, Z.-H., Lim, T.-T., 2014. Recent development of mixed metal oxide anodes for
687 electrochemical oxidation of organic pollutants in water. *Appl. Catal. A-Gen.* **480**, 58-78.

688 Xu, H., Li, A.-P., Qi, Q., Jiang, W., Sun, Y.-M., 2012. Electrochemical degradation of phenol on the
689 La and Ru doped Ti/SnO₂-Sb electrodes. *Korean J. Chem. Eng.* **29**, 1178-1186.

690 Yan, W., Fan, C.-M., Bo, H., Liang, Z.-H., Sun, Y.-P., 2009. Photoelectrocatalytic activity of two
691 antimony doped SnO₂ films for oxidation of phenol pollutants. *T. Nonferr. Metal Soc.* **19**, 778-
692 783.

693 Yang, S.Y., Choo, Y.S., Kim, S., Lim, S.K., Lee, J., Park, H., 2012. Boosting the electrocatalytic
694 activities of SnO₂ electrodes for remediation of aqueous pollutants by doping with various metals.
695 *Appl. Catal. B: Environ.* **111**, 317-325.

696 Yang, X., Kirsch, J., Fergus, J., Simonian, A., 2013. Modeling analysis of electrode fouling during
697 electrolysis of phenolic compounds. *Electrochim. Acta* 94, 259-268.

698 Yang, X., Zou, R., Huo, F., Cai, D., Xiao, D., 2009. Preparation and characterization of Ti/SnO₂-
699 Sb₂O₃-Nb₂O₅/PbO₂ thin film as electrode material for the degradation of phenol. *J. Hazard.*
700 *Mater.* 164, 367-373.

701 Yao, P., 2011. Effects of Sb doping level on the properties of Ti/SnO₂-Sb electrodes prepared using
702 ultrasonic spray pyrolysis. *Desalination* 267, 170-174.

703 Zhang, C., Du, X., Zhang, Z., Fu, D., 2016. The peculiar roles of chloride electrolytes in BDD anode
704 cells. *RSC Adv.* 6, 65638-65643.

705

706

707

708

709

710

711

712

713

714

715

716

717

718

719

720

721

722

723

724

725

726

727

728

729

730

731

732

Figure Captions

733

734

735 **Fig. 1.** (a) Cyclic voltammograms for the Ti/SnO₂-Sb anode produced using a conventional
736 furnace and (b) using alternative laser heating recorded at 50 mV s⁻¹ and (c) Nyquist plots for
737 the Ti/SnO₂-Sb anode produced using a conventional furnace and (d) using alternative laser
738 heating recorded at 1.7 V vs. Ag/AgCl and (e) service lifetime of anodes in the 0.1 M Na₂SO₄
739 background electrolyte.

740

741 **Fig. 2.** (a) Influence of supporting electrolyte on the removal of phenol as a function of
742 electrolysis time and (b) TOC removal after 60 min of treatment in the Na₂SO₄ 0.1 M and
743 with the addition of distinct concentration of NaCl in the supporting electrolyte. Conditions:
744 [Phenol₀]: 50 mg L⁻¹; pH: 6; applied voltage: 8 V. Inset: Pseudo-first-order kinetics for the
745 removal of phenol.

746

747 **Fig. 3.** (a) Phenol removal as a function of the electrolysis time, varying pH values at a fixed
748 applied potential of 8 V and (b) corresponding TOC removal after 60 min of treatment of
749 potential applied; (c) Phenol removal as a function of the electrolysis time, varying the
750 different potential applied at fixed pH: 6 and (d) corresponding TOC removal after 60 min of
751 the treatment. [Phenol₀]: 50 mg L⁻¹; Electrolyte: 0.03 M NaCl + 0.1 M Na₂SO₄

752

753 **Fig. 4.** (a) Phenol removal as a function of electrolysis time and initial phenol concentration
754 and (b) TOC removal during the treatment in the 0.30 M NaCl + 0.1 M Na₂SO₄ varying the
755 potential applied. Conditions: pH: 6, E: 8 V.

756

757 **Fig. 5.** HPLC chromatograms analyzed using a reversed-phase C18 column, UV detection at
758 254 nm as a function of electrolysis time during the treatment in the Na₂SO₄ 0.1 M using
759 conventional (a) and laser-made anode (c) and in Na₂SO₄ 0.1 M with the addition of 0.03 M
760 of NaCl using conventional (b) and laser-made anode (d). Conditions: [Phenol₀]: 50 mg L⁻¹,
761 pH: 6; applied voltage: 8 V, t = 60 min.

762

763